ELSEVIER

Journal of Alloys and Compounds 229 (1995) 54–65

Journal of ALLOYS AND COMPOUNDS

Solid state chemistry and luminescence of X-ray phosphors

S.L. Issler[a], C.C. Torardi[b,*]

[a]*Medical Products, DuPont Company, Wilmington, DE 19880-0352, USA*

[b]*Central Research and Development, DuPont Company, Experimental Station, Wilmington, DE 19880-0356, USA*

Received 10 March 1995

Abstract

X-ray phosphors are solid state inorganic materials used in medical X-ray imaging applications. The role of these phosphors is to reduce the exposure of the patient to X-rays while maintaining the structural features of the X-ray image. This is done by amplifying every X-ray photon absorbed by a phosphor screen into hundreds of visible- or UV-light photons which are then recorded by a detector, such as a piece of photographic film. Conventional screen/film imaging methods, still the highest quality, most widely used, and most cost effective diagnostic tools in radiology, are emphasized. A good X-ray phosphor must meet challenging prerequisites: good X-ray absorption in the diagnostic medical energy range (15–100 keV), high luminescence efficiency, emission in the green to near-UV region, proper crystallite size and shape, air and water stability, and easy large-scale production. The commercially important X-ray phosphors (e.g., LaOBr:Tm, Gd_2O_2S:Tb and M′–$YTaO_4$) are all synthesized by high-temperature reactions (800–1300°C) in the presence of a flux. The chemistry and properties of these phosphor compounds and recent discoveries in reaction chemistry are discussed. Research on new X-ray phosphors is also described.

Keywords: Solid state chemistry; Luminescence; X-ray phosphors

1. Introduction

A phosphor is a material that emits light as a result of it absorbing energy (Fig. 1). Luminescence is the term given to the emission of this light. The excitation energy (i.e., the energy absorbed) may be supplied in various forms. If photons of visible or ultraviolet light are used for excitation, the emission of light is called photoluminescence. If excited by electrical energy, the phosphor is called electroluminescent. Electrons result in cathodoluminescence, physical impact gives rise to triboluminescence, and heating a phosphor to release energy held in "traps" yields thermoluminescence. Therefore, an X-ray phosphor is a material that emits light when excited with X-rays, although it may also be stimulated with lower energy sources such as electrons or photons of ultraviolet light. General perspectives of the luminescence of solids can be found in textbooks [1–3] and recent reviews [4–7].

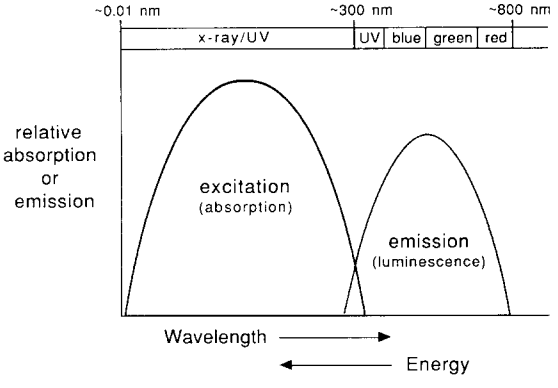

Fig. 1. Diagram illustrating the energy absorbed by a phosphor (left), which is then transformed to emitted light of lower energy (right).

In medical X-ray imaging, X-ray phosphors (sometimes referred to as scintillators) are used in film/screen cassettes [8]. Phosphors are also used in the detectors found in electronic systems such as computed radiography (CR) [1,9,10], computed tomography (CT) [1,11], fluoroscopy [10], and phosphor/CCD (charge coupled device) array detectors [12]. This paper will focus on conventional X-ray phosphors employed in film/screen cassettes. Although this technology has been used since shortly after Roentgen discovered X-rays in 1895, medical film/screen systems

* Corresponding author.

SSDI 0925-8388(95)01686-4

are still the most widely used diagnostic devices. They provide the highest quality of all medical imaging modalities, and remain the most cost effective diagnostic tools in radiology.

Most of us have gone to the hospital or doctor's office and had an "X-ray" taken of some part of the body. A thin plastic sheet coated on both sides with silver-halide emulsion, i.e., the X-ray film, is inserted into a cassette (Fig. 2). When the cassette is closed, a screen, consisting of a plastic sheet coated with an X-ray phosphor, is pressed against each side of the X-ray film. The patient is situated between the X-ray source and the cassette. The section of the body to be imaged is placed in contact with the cassette. X-rays travelling through the body are absorbed and scattered by bones and tissue to differing degrees and, as a result, a structural image is carried by the X-rays reaching the cassette. Most of these X-ray photons are absorbed by the front and back phosphor screens. The screens "intensify" the image by converting each absorbed X-ray photon into hundreds or thousands of ultraviolet–or visible-light photons that form the latent image in the silver halide emulsion. The role of the phosphor is, therefore, to reduce the patient's exposure to X-rays. To obtain a good image on X-ray film without phosphor screens would require an unacceptably high X-ray exposure (30–50-times) of the patient.

However, the sharpness of the X-ray image arriving at the cassette is reduced by both the screen and the film. This is due to light diffusion in the screen, and to print-through (also called cross-over) in the film (Fig. 3). In the screen, each phosphor particle emits radially. The emitted photons are scattered off neighboring

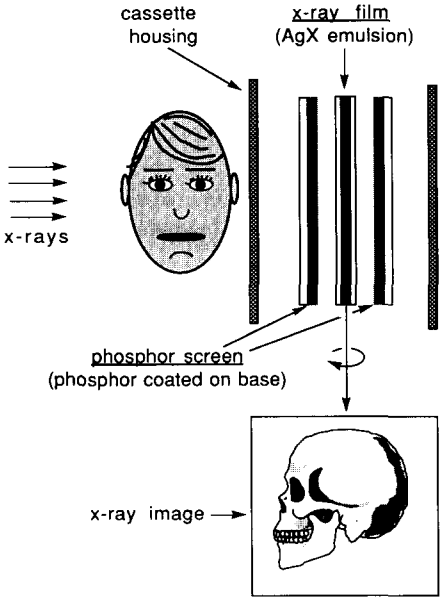

Fig. 2. Schematic diagram of a screen/film cassette used in medical X-ray imaging. Individual components shown separated for clarity.

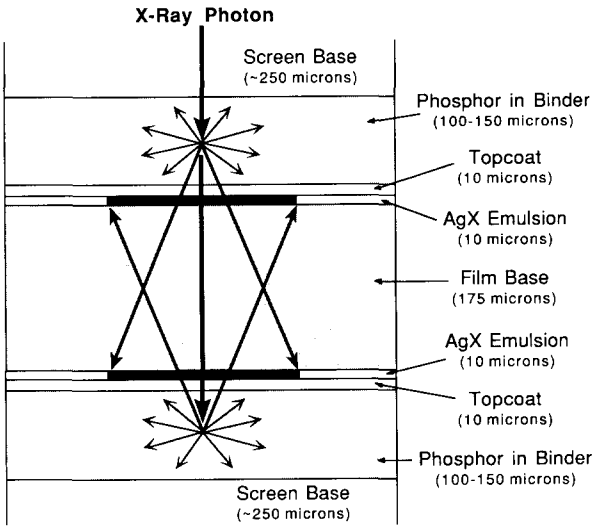

Fig. 3. Schematic cross-section of a two-screen/double-sided film system illustrating the paths of emitted photons within the phosphor screen and the "cone" of photons that escape the screen to expose the AgX film.

phosphor crystals prior to exiting the screen and exposing the photographic emulsion. A portion of these emitted photons is attenuated within the screen. A "cone of emission" is often used to describe the distribution of actinic light photons that reach the X-ray film. Print-through occurs in visible-light emitting screens when a fraction of the light emitted by one screen transmits through the film to the emulsion on the opposite side. Because the film base is relatively thick, the emission from the screen continues to spread as it passes through the base, causing further reduction in the sharpness of the image. Print-through can occur from both the front and back screens. Green light emitting screens can print-through up to 40% of their emitted light, and blue-emitting screens can print-through up to 30%.

Therefore, a compromise must be made between the minimum patient X-ray dose and the maximum diagnostic accuracy (image quality) when using medical X-ray film/screen systems.

A phosphor screen consists essentially of three layers (Fig. 3). A sheet of base material, often polyethylene terephthalate, is coated with a layer of X-ray phosphor mixed with a polymeric binder. A plastic topcoat is added to protect the phosphor layer from abrasion, dirt, etc. A reflecting material, such as TiO_2 or $BaSO_4$, may be coated on or incorporated into the base layer to reflect light towards the X-ray film. Phosphor screens are used many times and can last for years. Each piece of X-ray film is used only once.

In the phosphor screen, we need to capture as many of the incoming X-rays as possible in order to maintain a short exposure, and not allow the structural in-

formation to get lost by travelling clear through the cassette. Therefore, an X-ray phosphor must be a good absorber of X-rays. It is a high-density compound containing elements with high atomic numbers such as $CaWO_4$, $YTaO_4$, Gd_2O_2S, and LaOBr. Of course, the phosphor must also intensify the X-ray image by fluorescing many visible- or UV-light photons per X-ray photon absorbed, meaning that the phosphor must have good X-ray-to-light conversion efficiency, or "speed". Efficiencies generally run in the range 5–20% on the basis of the UV- or visible-light energy released versus the X-ray energy absorbed by the phosphor. Most of the absorbed energy is lost thermally.

X-ray intensifying phosphor screens are important to companies such as DuPont, Kodak, 3M, Agfa, Fuji and Konica because they support a large business, mainly in the sale of silver-halide X-ray films. Examples of commercially available X-ray phosphors are blue-emitting $CaWO_4$ and LaOBr:Tm, green-emitting Gd_2O_2S:Tb, and ultraviolet-light emitting $YTaO_4$. The chemistry of these compounds is discussed in more detail below.

The goal of X-ray phosphor research is to design materials that will lower X-ray exposure and improve image quality. At DuPont, the X-ray phosphor research program is composed of several parts. One part is the study of the chemistry of phosphor synthesis with the goal of making better materials. Another part is the exploratory search for new phosphors, both as totally new compounds and for making existing compounds fluoresce efficiently. A third part is to study the relationships between the luminescence and crystal and electronic structures.

We start with a brief introduction to solid-state chemistry, inorganic luminescence, and the history of X-ray phosphors. This is followed with a description of the synthesis of today's best X-ray phosphors. Next, reaction chemistry studies are discussed that have led to a different way of thinking about fluxes (described below) in solid state syntheses. Then, phosphor chemistry that has allowed the facile synthesis of traditionally "hard-to-make" compounds is described. Finally, some work in the area of new X-ray phosphors is presented.

2. Background

2.1. Solid state chemistry

Solid state chemistry [13–15] involves the synthesis, structure, properties, and applications of solid inorganic materials such as oxides, halides, sulfides, and intermetallics. These inorganic compounds almost always have long-range bonding, i.e., they are non-molecular, and their structures are derived by the manner in which the atoms are arranged in the three-dimensional solid. It is important to understand that the properties of solid state compounds are determined by their crystal structure and bonding.

Another important aspect of solid state chemistry is the defect structure of solids [13–15]. Structural defects influence the properties of solids such as electrical resistivity (insulator to metal), mechanical strength (iron vs. steel), and chemical reactivity (catalysts). Defects in solids can be of different types, but point defects, occurring at a position or "point" in the structure, are most common. For example, an atom in the host compound may be missing (a vacancy), or replaced with a different atomic element (a substitutional dopant or impurity) as shown in Fig. 4. Many X-ray phosphors luminesce efficiently only when substitutional dopants are incorporated into the structure.

Solid state compounds are synthesized by a variety of techniques. Two of the most common are solid state reaction and molten flux synthesis [2,14,15]. Solid state reactions, or the ceramic method, usually involve powders of the starting materials that are first intimately mixed, then heated to induce atomic diffusion. Molten flux reactions have included a material that is molten at the reaction temperature that aids diffusion of the reactants. As we will see, all of the important commercially manufactured X-ray phosphors are synthesized via the molten flux procedure. To analyze and study solid state compounds, X-ray and electron diffraction are common, as well as other electron microscopic techniques [14].

2.2. Inorganic luminescence

Photoluminescent materials require a host crystal structure such as ZnS, Al_2O_3, $CaWO_4$, and $YTaO_4$

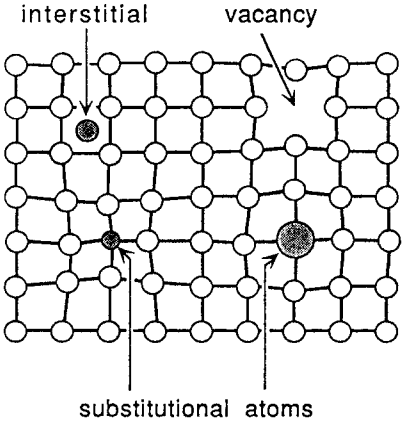

Fig. 4. A two-dimensional illustration of some point defects that occur in solids.

and an activator such as Mn^{2+}, Sn^{2+}, Eu^{3+}, and Ti^{4+}. Activators are commonly transition metal, main group, or rare earth ions. The activator is a dopant that creates substitutional defects in the host structure. The formulas of doped compounds may be represented as, for example, ZnS:Mn or $Zn_{1-x}Mn_xS$ where x is often less than about 0.1. Note that luminescence comes from the activator. These inorganic luminescent materials are known generally as phosphors. A phosphor is said to exhibit fluorescence if the time between excitation (i.e., absorption of energy by the activator) and emission is in the range 10^{-9} to 10^{-3} seconds [2]. Emission occurring with longer decay times is referred to as phosphorescence. The activator may absorb the excitation energy directly, thereby promoting an electron from the atom's ground state to excited states, or the energy may be transferred from the host to the activator as in X-ray phosphors.

Host materials used for X-ray phosphors are white, ionically bonded, insulating compounds with band gaps in the ultraviolet region. The activator has discrete energy levels associated with it and these levels are modified to different degrees depending on the type of activator and the local environment of the host structure. For example, activator ions that feel only a small influence from the host lattice will luminesce with narrow line emission characteristic of that particular activator atom. This narrow line emission is common for rare earth activators such as Tb^{3+}, Tm^{3+}, or Eu^{3+} whose optical transitions involve only f-orbital energy levels. When the energy levels of activator ions are strongly modified by the host structure, the emission transitions of the activator are generally of a more complicated nature and are often only partially understood. Strong influence by the host lattice most often causes these activators to luminesce with broad band emission. An example of an activator that emits broad blue emission is Nb^{5+}. Also, the same activator ion in two different host structures that significantly modify the energy levels of the activator may luminesce with a particular color in one host, and emit a different color from the other host. The activator ions Ce^{3+} or Bi^{3+} are broad band emitters whose peak emission intensity can be located at different wavelengths in different host structures.

To understand the luminescence processes in ionically bonded phosphors, the configurational coordinate diagram is used [1,3,14,16] (Fig. 5). The activator is excited from its ground state (A) to a higher energy level (B). Some of this absorbed energy is given up to the host structure as heat, and the activator ion relaxes to a lower energy excited state (C). The activator then returns to the ground state (A), releasing its energy by emitting light. Note that the energy of excitation is greater than the energy of emission. The decrease in energy, or the increase in wavelength, is known as the Stoke's shift.

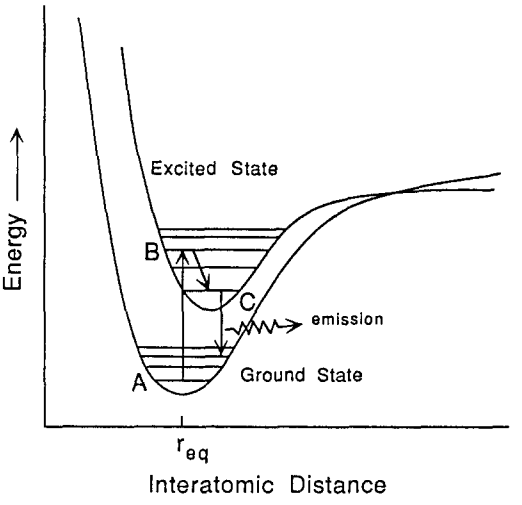

Fig. 5. Example of a configurational coordinate diagram used to qualitatively understand luminescence in phosphors. Shown is the excitation of an electron from ground (A) to excited state (B), relaxation of the excited state electron to a lower energy excited state (C) and return to the ground state with emission of light .

To study phosphor luminescence under X-ray excitation, equipment such as that illustrated in Fig. 6 is used. Polychromatic X-radiation, 1, bombards the sample, 2. Some of the emitted light passes through focusing lenses, 3, to a photomultiplier, 4, used to record the amount of emitted light, 6. This is compared to the emission level of a standard, often $CaWO_4$. Emitted light is also focused into a monochrometer, 5, to obtain the spectrum of the emission, 7.

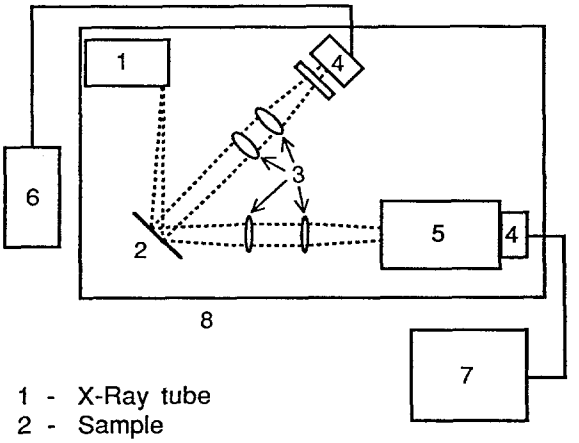

Fig. 6. Schematic of the experimental equipment used in the study of phosphors under X-ray excitation.

2.3. Requirements for a good X-ray phosphor

There are several important requirements for a good X-ray phosphor. It must strongly absorb X-rays, particularly the polychromatic X-ray photons in the 15–100 keV energy range (e.g., tungsten X-rays) used in medical radiography. High X-ray absorption is necessary to minimize patient X-ray exposure and to maximize the signal-to-noise ratio for optimal image quality [10]. Strong X-ray absorption occurs in compounds containing elements with K-edges (i.e., X-ray energy required to remove a 1s electron) in the diagnostic X-ray energy range. Fig. 7 shows the absorption of several X-ray phosphors as a function of X-ray photon energy, clearly showing the K-edge absorption of the heavy elements in the host structure.

The luminescence efficiency (i.e., X-ray-to-light conversion efficiency) of the X-ray phosphor must also be high to maximize imaging speed and to minimize patient exposure. Typical luminescence efficiencies for commercial X-ray phosphors are 5–20%. Fluorescence, not phosphorescence, is the required type of luminescence and any delayed emission (i.e., "afterglow" or "lag") must be kept to a minimum or eliminated so that subsequent film exposures do not become "fogged" or contain images of the previous patient.

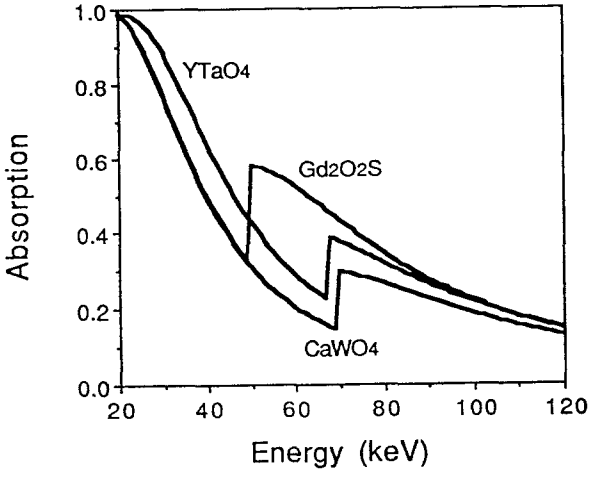

Fig. 7. Absorption of X-ray energy by phosphor screens (150 μm thick) showing the strong K-edge absorption of the heavy elements (i.e., Ta, Gd and W).

The wavelength of emission from the phosphor must spectrally fall in the X-ray film's absorption energy region to maximize the imaging speed of the film/screen system. Silver halide particles commonly used in photographic film have an intrinsic absorption in the blue and ultraviolet energy region. However, silver halide films can be altered to absorb light from green-emitting X-ray phosphors by using sensitizing dyes.

Luminescence efficiencies are related to the phosphor crystallite size with the optimum size being in the 2 to 12 μm range. Smaller crystals are less efficient because of lower bulk emission intensity. Also, tighter packing of the smaller particles will increase the probability that the emitted light will get lost (attenuated) within the screen. Larger crystals cause difficulties in coating the phosphor particles into smooth, thin screens.

To maximize the sharpness of X-ray images, it is important to make the screen coatings as thin as possible with a dense packing of the phosphor powder. Therefore, phosphor particles of roughly spherical shape with relatively high densities, greater than 6 g cm^{-3}, are preferred.

Phosphor particles should also be air and water stable, and prepared using a straightforward, cost-effective commercial process. Radioactive isotopes must not be present in X-ray phosphors since radioactivity will fog the X-ray film.

2.4. History of X-ray phosphors

X-rays were discovered by Wilhelm Conrad Roentgen in 1895. In the following year, $CaWO_4$ was found to intensify the light output of X-rays. This phosphor was used almost exclusively for 75 years. In the early 1970s came the discovery of the "rare-earth" phosphors. The rare-earth phosphors gave researchers the ability to engineer new phosphors with greater density and improved X-ray absorption (Fig. 7) and higher X-ray-to-light conversion efficiencies. Today's best X-ray phosphors are given in Table 1, which includes

Table 1
Properties of commercial X-ray phosphors

Phosphor	Conversion efficiency (%)	Density (g cm^{-3})	K-edge (keV)	Emission (color, width)
$CaWO_4$	5	6.12	70	blue, broad
BaFCl:Eu	16	4.56	37	UV/blue, broad
LaOBr:Tm	18	6.10	40	UV/blue, line
Gd_2O_2S:Tb	19	7.34	50	green, line
M′–$YTaO_4$	8	7.57	67	UV, broad
M′–$YTaO_4$:Nb	8	7.57	67	blue, broad

$CaWO_4$ for comparison. All of these phosphors are prepared at temperatures greater than 800°C by flux synthesis.

A flux is defined [2] as "a material which melts lower than the solid state reaction temperature, dissolves one or more of the components and allows material transport to the reaction zone, without entering into the solid state reaction. Preferably, the end-product should be insoluble in the flux". However, as will be seen below in Section 4.2, the flux can be more intimately involved in the formation of the product.

3. Commercial X-ray phosphors: synthesis and properties

A brief description of the syntheses and crystal structures of the phosphors in Table 1 is now given. X-ray excited emission spectra are also presented. A more detailed description of the history of these compounds as well as image quality data is given in Ref. [8].

3.1. $CaWO_4$

$CaWO_4$, also known by its mineral name scheelite, crystallizes with tetragonal symmetry ($a = 5.243$ and $c = 11.374$ Å) and has a density of 6.12 g cm^{-3}. It contains isolated tetrahedral WO_4^{2-} groups interconnected by calcium ions in 8-coordination with oxygen [17] (Fig. 8). Synthesis is as follows:

$$Na_2WO_4 + CaCl_2 \xrightarrow{900\,^{\circ}C} CaWO_4 + 2NaCl$$

NaCl formed in the reaction acts as a flux to produce round polyhedral crystallites. Pure calcium tungstate suffers from high lag (afterglow), and a small amount of sulfate is added to the reaction, as $NaHSO_4$, to lower the afterglow. Mechanisms for lag are not well understood, and consequently the required chemistry necessary to control lag is determined by much trial-and-error. $CaWO_4$ emits broad band blue light with the maximum in the emission peak at 430 nm (Fig. 9). Emission is understood to be from the tungstate group [18], and $CaWO_4$ is thus referred to as being "self activated". Because of its inferior X-ray absorption relative to newer materials, the use of $CaWO_4$ as a phosphor has decreased considerably in the recent years.

3.2. BaFCl:Eu

One of the first rare-earth X-ray phosphors was BaFCl:Eu. The host, BaFCl, is a layered material having the tetragonal PbFCl structure with $a = 4.393$ and $c = 7.225$ Å and $\rho = 4.56$ g cm^{-3} [19]. Individual

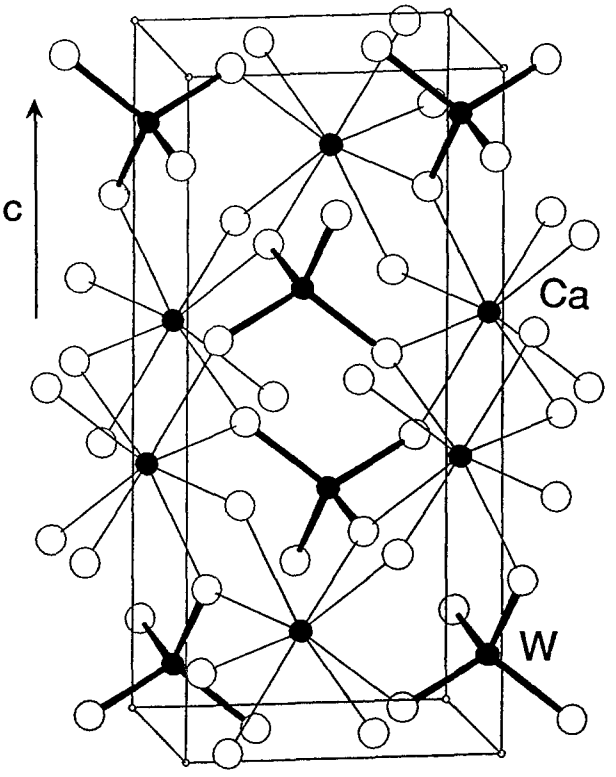

Fig. 8. Structure of tetragonal $CaWO_4$ (scheelite) showing the isolated tetrahedral WO_4 units interconnected by 8-coordinated Ca ions. Ca and W are shaded.

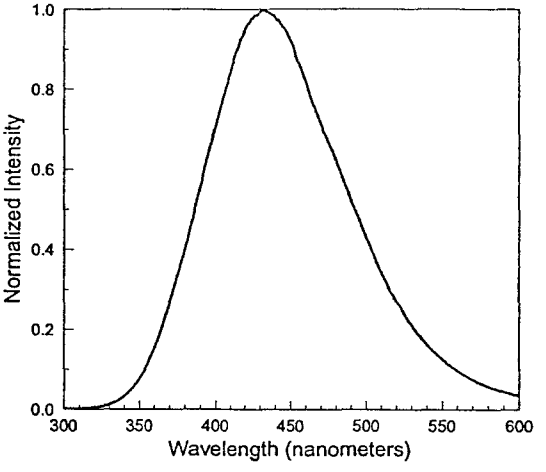

Fig. 9. Broad band emission spectrum of $CaWO_4$ (scheelite) peaking in the blue region (430 nm) under X-ray excitation (Mo 30 kVp (peak kilovoltage)).

layers contain BaF_4Cl_4 square antiprisms that share edges and faces within the layer and are arranged to have the fluoride and chloride anions located in the middle and outer parts of the layer, respectively (Fig. 10). In addition, each Ba atom bonds to a chlorine atom in an adjacent layer, making the barium nine-coordinated (4 F and 5 Cl atoms). The latter bond holds the layers together. Europium, the activator,

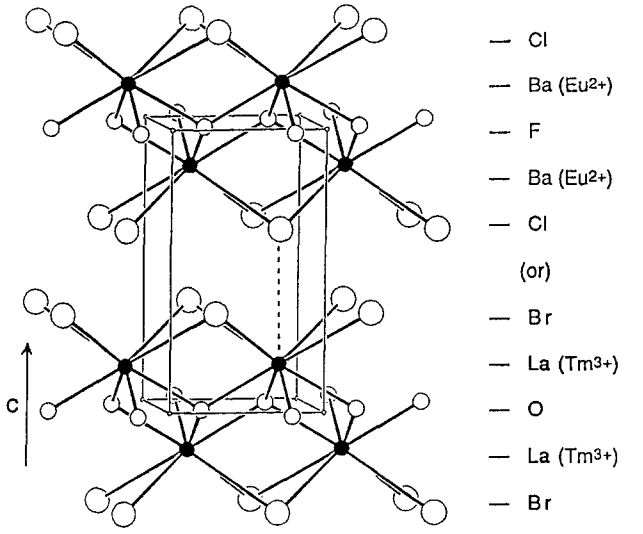

Fig. 10. Tetragonal structure of the layered compounds BaFCl and LaOBr showing the smaller F or O ions in the middle of the layer and larger Cl or Br ions forming the surface of the layers. One of the interlayer M–X bonds is shown as a dashed line. Metal atoms are shaded.

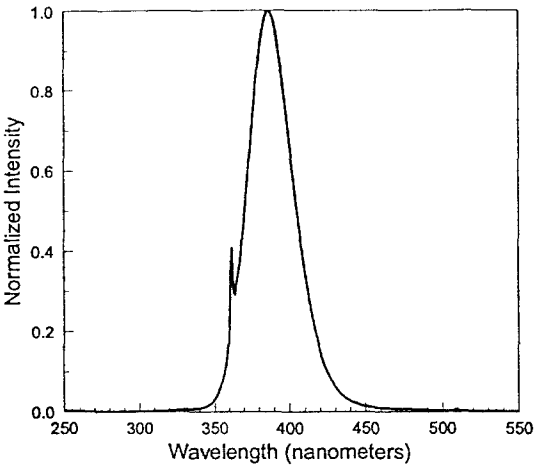

Fig. 11. X-ray excited (Mo 30 kVp) emission spectrum of europium in BaFCl:Eu showing its peak in the blue/near-UV energy region (390 nm).

substitutes for a small amount of the barium, giving the formula $Ba_{0.99}Eu_{0.01}FCl$ as the optimum composition. A fine powder is first precipitated from aqueous solution by stirring overnight the following:

$$(1-2x)BaF_2(s) + BaCl_2(aq) + 2x\ EuF_2(s) \xrightarrow{x\sim 0.01} 2\ Ba_{1-x}Eu_xFCl(s)$$

A stoichiometric excess of aqueous $BaCl_2$ solution is used. At this point, the precipitate may be separated, blended with $BaCl_2$ to serve as a flux, and fired. However, a product with plate-shaped crystallites is produced with this procedure. This undesirable morphology can be circumvented by spray drying the slurry of BaFCl:Eu and aqueous $BaCl_2$, heating the resulting well-mixed phosphor/flux intermediate at 1000°C, and finally washing out the $BaCl_2$ flux [20]. Under X-ray excitation, BaFCl:Eu emits in the blue/UV at 390 nm [21] (Fig. 11). At the time of its discovery, BaFCl:Eu was an improvement over $CaWO_4$ in speed by a factor of ~2. Even though the density of BaFCl is considerably lower than that of $CaWO_4$, the higher absorption in the 40–70 keV region makes the overall absorption about the same as that of $CaWO_4$. However, increasing speed with no increase in X-ray absorption produces images with lower signal-to-noise ratios because the image is created with fewer absorbed X-ray photons. For this reason BaFCl:Eu was abandoned for better materials, which are now described.

3.3. LaOBr:Tm

The very important phosphor LaOBr:Tm is isostructural with BaFCl and has higher absorption and density, 6.10 g cm^{-3}. The tetragonal unit cell parameters are $a = 4.159$ and $c = 7.392$ Å [22]. The smaller, more ionic oxide anion resides in the middle of the layer, and the bromide anions form the top and bottom of the layer (Fig. 10). The stacked layers are held together mainly by the interlayer La–Br bond. Thulium serves as the luminescent center in this efficient phosphor at a low dopant level, $La_{0.998}Tm_{0.002}OBr$. The synthesis is a bit more delicate than those of other phosphors owing to the sensitivity of bromide to water and to volatilization at high temperatures, but these complications have been overcome. It is synthesized as follows:

$$(1-x)La_2O_3 + xTm_2O_3 + 2\ NH_4Br \xrightarrow[\text{KBr flux}]{800\ ^\circ C} 2\ La_{1-x}Tm_xOBr + 2\ NH_3 + H_2O$$

Ammonium bromide serves as the brominating agent, while potassium bromide acts as the flux [23]. The problem of sensitivity to water vapor was solved by adding potassium antimony tartrate to the final product [24]. The crystallite morphology of LaOBr is plate-like, and there have been no process improvements to synthesize a more isotropic particle, as was done for BaFCl. Nevertheless, the superior properties of LaOBr:Tm allow its use in X-ray phosphor screens. Tm^{3+} emits predominantly in the UV and blue with several f–f electronic transitions observed [25] (Fig. 12).

3.4. Gd_2O_2S:Tb

One of the best known phosphors is hexagonal (trigonal) Gd_2O_2S:Tb ($a = 3.851$ and $c = 6.667$ Å [26]). It has high density, 7.34 g cm^{-3}, and, more important-

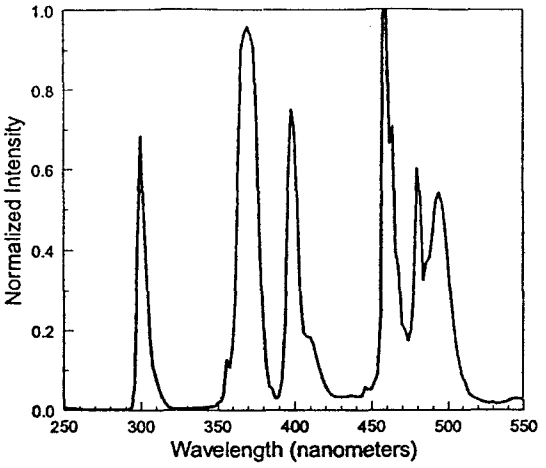

Fig. 12. Line emission spectrum of thulium in LaOBr:Tm under X-ray excitation (Mo 30 kVp) showing the predominant peaks in the UV and blue-light energy range (<500 nm).

ly, it has strong X-ray absorption at the Gd K-edge, 50 keV, which lies in the middle of the diagnostic X-ray energy range (Fig. 7). The structure (Fig. 13) is built of edge-sharing monocapped trigonal antiprisms composed of GdO_4S_3 units [27]. This host phase is synthesized by reacting the rare-earth oxides with sulfur in a polysulfide flux [28]:

$$Gd_2O_3 + x\,Tb_4O_7 + \text{excess S} \xrightarrow[1100\,^{\circ}C]{\text{polysulfide flux (S, } Na_2CO_3)} Gd_2O_2S{:}Tb^{3+} + \text{byproducts}$$

After washing, the phosphor is recovered as well-faceted round-shaped crystallites [8]. Although other trivalent rare-earth activators will luminesce in this host, Tb^{3+} doping creates one of the most efficient X-ray phosphors (19%) at $x \sim 0.01$. At this activator level, Gd_2O_2S:Tb emits predominantly green light as seen in the narrow line emission spectrum in Fig. 14. However, the "color" is dependent on the terbium concentration level, and a shift to blue emission occurs as x decreases because the emission peaks in the region below 500 nm increase in intensity [8].

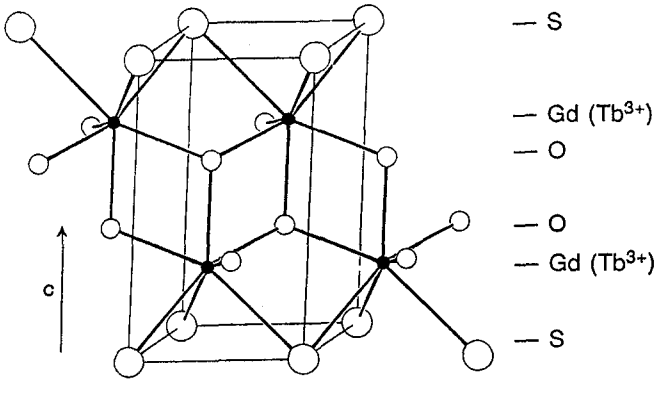

Fig. 13. Hexagonal (trigonal) structure of Gd_2O_2S showing positions of Gd, S and O atoms. Gd (shaded) is bonded to four oxygen and three sulfur atoms.

3.5. $YTaO_4$

One of the more recently commercialized X-ray phosphors is M′–$YTaO_4$ [29,30]. $YTaO_4$ exhibits three crystal structures. A high temperature tetragonal form (T) with the scheelite structure (as discussed for $CaWO_4$) distorts via a second-order phase transition to a monoclinic (M) structure having the fergusonite structure. Another monoclinic structure, called M′, can be synthesized directly at lower temperatures (below ~1400°C). M′ transforms to T at approximately 1450°C and then to M upon cooling. It is the M′ modification that is used in phosphor screens. The unit cell parameters are $a = 5.30$, $b = 5.45$, $c = 5.11$ Å and $\beta = 96.5°$, and the density is 7.57 g cm^{-3}. Tantalum is in a 4 + 2 coordination environment [29] with oxygen (Fig. 15). These distorted TaO_6 units share edges with one another to form strings. Yttrium, in eight-fold coordination with oxygen, interconnects the Ta–O strings.

The use of a flux in the synthesis of M′–$YTaO_4$ not only allows the growth of polyhedral, equi-axed, 4–12 μm single crystals, but also assists greatly in the formation of the compound [8]. Without a flux, it is necessary to heat at >1300°C several times with intermediate grindings. Using Li_2SO_4 or LiCl as a flux facilitates the reaction:

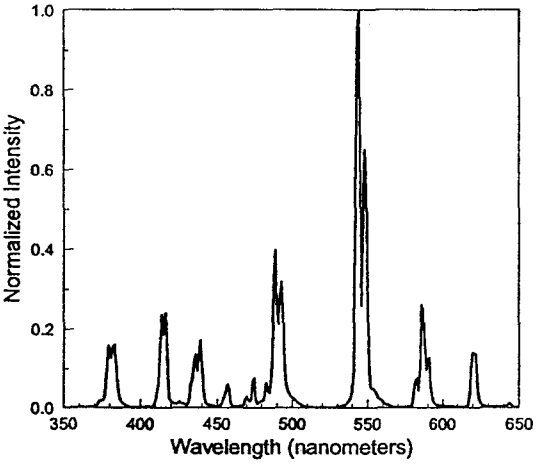

Fig. 14. Line emission spectrum of terbium in Gd_2O_2S:Tb under X-ray excitation (Mo 30 kVp) showing intense peaks in the green-light energy region (~545 nm).

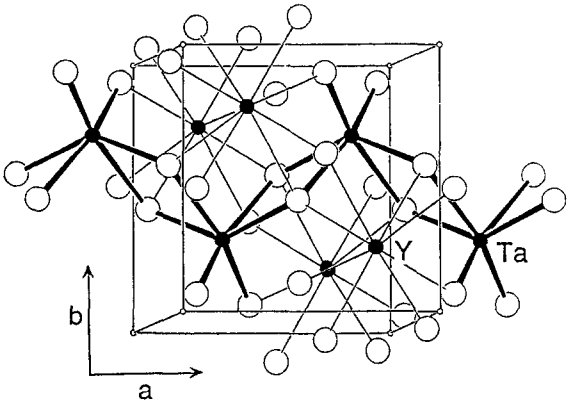

Fig. 15. Monoclinic structure of M′–$YTaO_4$ emphasizing a section of an edge-sharing chain of distorted TaO_6 units. Chains are interconnected by yttrium in 8-fold coordination with oxygen. Metal atoms are shaded.

$$Y_2O_3 + Ta_2O_5 \xrightarrow[1250\,^{\circ}C,\ 12\ h]{Li_2SO_4 \text{ or } LiCl} 2\,M'\text{–}YTaO_4$$

The chemistry involved in this reaction is discussed in more detail below. As in the case of $CaWO_4$, M′–$YTaO_4$ is self activated and emits broad band ultraviolet light peaking at 330 nm (Fig. 16). This compound is versatile because it can also be doped with other elements to make phosphors efficiently emitting different "colors". Activating with Nb, i.e., M′–$YTa_{1-x}Nb_xO_4$ with $x = 0.005$–0.020, shifts the emission from UV (330 nm) to blue (410 nm) [29] as seen in Fig. 16. The denser, isostructural compounds M′–$GdTaO_4$ and M′–$LuTaO_4$ offer improved X-ray absorption. The major drawback of the latter compound is its cost.

4. Recent developments in conventional X-ray phosphors

4.1. Ultraviolet-emitting X-ray phosphors

Recently, the use of UV-emitting X-ray phosphors such as M′–$YTaO_4$ in place of visible-light emitting phosphors in intensifying screens was found to significantly improve image sharpness in radiographs [30]. There are two reasons for the improvement in image quality. First, the UV light is more highly attenuated within the intensifying screen, especially at higher scattering angles relative to the direction perpendicular to the surface of the screen (Fig. 17). As a result, the image emanating from the screen (i.e., the cone of emission) will be sharper than that of comparable visible-light emitting screens. Secondly, print-through is virtually eliminated because the UV light emitted from the intensifying screen is more efficiently absorbed by the silver halide emulsion, and because any remaining UV light that transmits through the emulsion is attenuated by the film base.

The use of UV-emitting phosphors is a simple and highly effective way of significantly improving image quality in a radiograph. Since 1992, UV-emitting screen/film systems, covering all conventional X-ray imaging applications, have been commercialized by the DuPont Company under the name Ultra-Vision™ [30–32]. Because of this technological significance, recent R&D efforts have been focused on the search

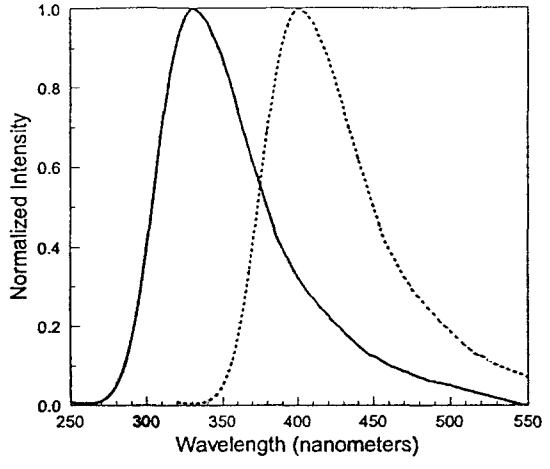

Fig. 16. X-ray excited (Mo 30 kVp) emission spectra of M′–$YTaO_4$ and M′–$YTa_{0.98}Nb_{0.02}O_4$ showing broad band UV emission centered at 330 nm (solid line) and blue emission centered at 410 nm (dashed line), respectively.

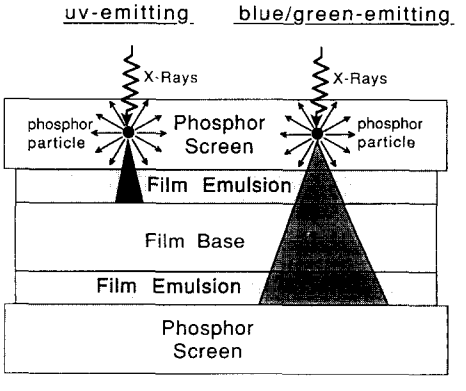

Fig. 17. Schematic diagram explaining the increase in image sharpness and resolution obtained with UV-emitting phosphor screens relative to blue- and green-emitting screens. A more focused "cone of emission" and low print-through are illustrated for the UV-emitting example (left). For clarity, only one of the two screens is shown emitting light.

for other UV-emitting X-ray phosphors (i.e., those with emission less than 400 nm).

4.2. Chemistry of phosphor synthesis

To understand better the dynamics of M′–$YTaO_4$ formation, the reaction chemistry was studied as a function of temperature [33,34]. Differential thermal analyses (DTA) display an exothermic peak when Y_2O_3, Ta_2O_5, and Li_2SO_4 (or LiCl) are reacted at elevated temperatures. No exothermic peak occurs in the absence of any one of the three starting ingredients. The exothermic process occurs at or very near to the melting point of the flux, 860°C for Li_2SO_4 and 610°C for LiCl. Note that melting is an endothermic event. X-ray powder diffraction patterns of samples quenched from various temperatures, and also recorded at temperature, reveal that the flux actually reacts with the starting oxides to form two intermediate compounds. For the general case of a rare-earth oxide, R_2O_3:

$$R_2O_3 + Ta_2O_5 + Li_2SO_4 \xrightarrow{\sim 850\,^\circ C} 2\ LiTaO_3 + R_2O_2SO_4$$

A small amount of these intermediate phases is visible via X-ray powder diffraction below the melting point of the Li_2SO_4. However, at the melting point of the flux, the crystallization of $LiTaO_3$ and $R_2O_2SO_4$ is accelerated, releasing energy as heat. As the temperature rises, the intermediates react slowly to make M′–$RTaO_4$ and to regenerate Li_2SO_4:

$$2\ LiTaO_3 + R_2O_2SO_4 \xrightarrow{850\text{–}1250\,^\circ C} 2\ M'\text{-}RTaO_4 + Li_2SO_4$$

At 1250°C, the Li_2SO_4 behaves as a flux, assisting in the growth of crystallites. Other sulfate compounds, e.g., Na_2SO_4 and K_2SO_4, also react to form intermediates [35]. Chloride compounds react with R_2O_3 and Ta_2O_5 to form oxychloride intermediates. For example:

$$R_2O_3 + Ta_2O_5 + 2\ LiCl \xrightarrow{\sim 610\,^\circ C} 2\ LiTaO_3 + 2\ ROCl$$

$$2\ LiTaO_3 + 2\ ROCl \xrightarrow{610\text{–}1200\,^\circ C} 2\ M'\text{-}RTaO_4 + 2\ LiCl$$

Looking only at the initial reactants and final products of the $RTaO_4$ reaction leads one to conclude that Li_2SO_4 and LiCl act as conventional fluxes as described earlier. However, in light of the new discovery, a more appropriate term for these compounds may be "catalyst" or "reactive flux" because they facilitate the synthesis of $RTaO_4$ through chemical reaction.

The importance of these findings is that a different way of thinking of the chemistry of fluxes in solid state syntheses has developed. This has allowed the facile synthesis of pure compounds that have traditionally been difficult to prepare [36]. Some examples of this chemistry, applied to the synthesis of potential phosphor hosts, follow.

4.3. Improved compound syntheses

Bismuth tantalate, $BiTaO_4$, exists in two structural modifications, a high temperature triclinic phase and a low temperature orthorhombic phase [37]. Long reaction times [37] and a colored product [38] are reported for $BiTaO_4$. Both the high and low temperature phases are easily synthesized [36] as white powders in 12 h at 1000°C and 900°C, respectively, using Li_2SO_4 as a "flux".

$$Bi_2O_3 + Ta_2O_5 \xrightarrow[Li_2SO_4]{900 \text{ or } 1000\,^\circ C,\ 12\ h} 2\ BiTaO_4$$

The reactions are done in air in covered alumina crucibles. Crystals are 2–10 μm in size. LiCl can not be substituted for Li_2SO_4 in this process because bismuth is lost, presumably as a volatile chloride-containing intermediate. $BiTaO_4$ has high density, 9.33 g cm^{-3}, and good X-ray absorption. Unfortunately, attempts to activate this host have been unsuccessful.

The cubic fluorite-related phases $R_2Hf_2O_7$ (R = rare-earth and yttrium) are reported to be made by solid state reaction of the constituent oxides above 1800°C [39]. The high temperature is required for the reaction to go to completion. The reaction temperature can be lowered considerably by the use of Li_2SO_4 as a reactive flux [36]. This is analogous to the situation found in the synthesis of M′–$YTaO_4$, but for $R_2Hf_2O_7$ the results are more dramatic. The synthesis temperature is lowered by over 700°C in the case of R = La:

$$La_2O_3 + 2\ HfO_2 \xrightarrow[Li_2SO_4]{1100\,^\circ C} La_2Hf_2O_7$$

The other rare-earth hafnate analogs are cleanly prepared at 1200°C using Li_2SO_4 [36].

4.4. New X-ray phosphors

Efficient X-ray phosphors, $Li_3Ta_{1-x}Nb_xO_4$, were synthesized during a study of the compounds that could form in the Y_2O_3, Ta_2O_5/Nb_2O_5, Li_2SO_4 or LiCl systems [36]. The phosphors are easily prepared using lithium sulfate flux in covered alumina crucibles:

$$3\ Li_2CO_3 + (1-x)\ Ta_2O_5 + x\ Nb_2O_5 \xrightarrow[Li_2SO_4]{1000\text{–}1100\,^\circ C,\ 12\ h} 2\ Li_3Ta_{1-x}Nb_xO_4 + 3\ CO_2$$

The low-temperature monoclinic crystal structure of Li_3TaO_4 [40] is observed for x up to 0.5. In this range, the wavelength of the broad-band emission peak under Mo X-ray excitation shifts from 410 nm at $x = 0$ to 435 nm at $x = 0.5$. The $x = 0$ compound exhibits

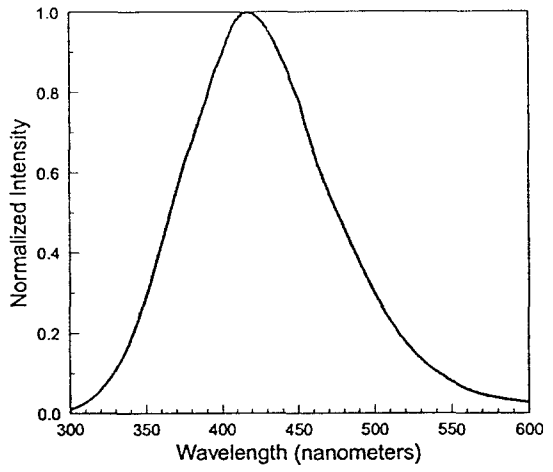

Fig. 18. X-ray excited (Mo 30 kVp) emission spectrum of $Li_3Ta_{0.998}Nb_{0.002}O_4$ showing broad band blue emission peaking at 415 nm.

speed comparable to that of $CaWO_4$. However, the brightest phosphor is found with $x \sim 0.005$ (Fig. 18). In the range $x = 0.5$–0.8, two structure types exist, monoclinic Li_3TaO_4 and cubic Li_3NbO_4. For $x > 0.8$, only the cubic Li_3NbO_4 structure is observed in X-ray powder diffraction patterns. Under the preparative conditions employed (1000°C), the solubility of Nb in the monoclinic Li_3TaO_4 structure is much greater than that of Ta in the cubic Li_3NbO_4 structure. Undoped Li_3NbO_4 emits at 405 nm under X-ray excitation. The UV-excited luminescence of the end members, Li_3TaO_4 and Li_3NbO_4 [41], has peak emission energies, 459 and 370 nm, respectively, which are different from those observed under X-ray stimulation. Blue-emitting Li_3TaO_4:Nb is a faster phosphor than $CaWO_4$, but it has about the same X-ray absorption, thereby making it less attractive for most medical imaging applications.

Several additional blue/UV emitting X-ray phosphors have been developed in recent years by the Eastman Kodak Company: $Mg_4Ta_2O_9$:Ti [42], HfO_2:Ti [43], Li_2HfO_3:Sn [44] and $HfGeO_4$:Ti [45]. The primary objective of this research has been to achieve a better spectral match between the intrinsic absorption of silver halide films and the emission of X-ray phosphors. The properties of these new materials are summarized in Table 2. HfO_2:Ti [46] and $HfGeO_4$:Ti [47] are promising phosphors for use in mammography screens. Large scale commercial manufacture using these phosphors in screen/film applications remains the challenge.

5. Summary

X-ray phosphors are technologically important materials used primarily for medical X-ray imaging applications. The role of these phosphors is to reduce the exposure of the patient to X-rays while maintaining the quality of the image. This is done by amplifying every X-ray photon absorbed by a phosphor screen into hundreds of visible- or UV-light photons which are then recorded by a detector, such as a piece of photographic film. Conventional screen/film imaging methods are still the highest quality, most widely used, and most cost effective diagnostic tools in radiology. Phosphors are composed of a host compound containing an activator (i.e., chemical element) from which light is emitted. The crystal structure and bonding within the host, as well as the nature of the activator, control the energies of the emitted light and the efficiency of these emissions. A good X-ray phosphor must meet strict prerequisites: good X-ray absorption in the diagnostic medical energy range (15–100 keV), high luminescence efficiency, emission in the green to near-UV region, proper crystallite size and shape, air and water stability, and easy commercial production. Employment of UV-emitting phosphors in screen/film systems significantly improves radiographic image sharpness.

All of the best known X-ray phosphors are synthesized at temperatures above 800°C with the use of a flux. The preparative chemistry and emission-related properties of the compounds $CaWO_4$, M′–$YTaO_4$, LaOBr:Tm, BaFCl:Eu, and Gd_2O_2S:Tb were discussed. Investigations of the reaction chemistry of M′–$YTaO_4$ formation from the oxide constituents in the presence of various fluxes have uncovered the dual role of the flux, first as a catalyst, by reacting with the starting oxides to produce reactive intermediate phases, and secondly as a flux, growing crystallites to the appropriate size and morphology. The chemistry

Table 2
New X-Ray phosphors (Eastman Kodak)

Host	Phosphor example	Density ($g\ cm^{-3}$)	Emission (color, width)
$Mg_4Ta_2O_9$	$Mg_4Ta_2O_9$:Nb	6.2	blue/UV, broad
HfO_2	$Hf_{1-z}Zr_zO_2$:Ti,Ln,M[a]	10.1	blue, broad
Li_2HfO_3	$Li_2Hf_{1-z}Zr_zO_3$:Sn,Ti,Ln[a]	6.6	blue, broad
$HfGeO_4$	$(Hf_{1-z}Zr_z)_{1+x}Ge_{1-x}O_4$:Ti	8.5	blue, broad

[a]Ln = at least one rare earth element, and M = at least one alkali metal.

learned from these studies has been extended to the synthesis of other traditionally "hard-to-make" compounds such as $BiTaO_4$ and $La_2Hf_2O_7$.

New X-ray phosphors have recently been prepared and were discussed. The most promising of these new phosphors include broad band, blue-emitting $Li_3Ta_{1-x}Nb_xO_4$, HfO_2:Ti and $HfGeO_4$:Ti.

Acknowledgements

The authors thank C. Roger Miao, Dr. Paul D. VerNooy and Chan Suto for helpful suggestions on this paper.

References

[1] G. Blasse and B.C. Grabmaier, *Luminescent Materials*, Springer Verlag, Berlin, 1994.
[2] R.C. Ropp, *Luminescence and the Solid State*, Elsevier Science, Amsterdam, 1991.
[3] F.A. Kröger, *Some Aspects of the Luminescence of Solids*, Elsevier, Amsterdam, 1948.
[4] G. Blasse, *J. Alloys Comp., 192* (1993) 17.
[5] T. Welker, *J. Luminesc., 48/49* (1991) 49.
[6] G. Blasse, *Chem. Mater., 1* (1989) 294.
[7] H.G. Brittain, Application of lanthanide ion luminescence from inorganic solids, in S.J. Schulman (ed.), *Molecular Luminescence Spectroscopy: Methods and Applications — Part II*, John Wiley and Sons, New York, 1988.
[8] L.H. Brixner, *Mater. Chem. Phys., 16* (1987) 253.
[9] M. Sonoda, M. Takano, J. Miyahara and H. Kato, *Radiology, 148* (1983) 833.
[10] T.S. Curry III, J.E. Dowdey and R.C. Murry, Jr., *Christensen's Physics of Diagnostic Radiology*, Lea and Febiger, 4th edn., 1990.
[11] C.D. Greskovich, D. Cusano, D. Hoffman and R.J. Riedner, *Amer. Ceram. Soc. Bull., 71* (1992) 1120.
[12] H. Roehrig, W.S. Schempp, L.L. Fajardo and T. Yu, *Soc. Photo-Optical Instrum. Eng. (SPIE), Med. Imaging, 2163* (1994) 33.
[13] L. Smart and E. Moore, *Solid State Chemistry — An Introduction*, Chapman and Hall, 1992.
[14] A.R. West, *Solid State Chemistry and Its Applications*, John Wiley and Sons, New York, 1990.
[15] C.N. R. Rao and J. Gopalakrishnan, *New Directions in Solid State Chemistry: Structure, Synthesis, Properties, Reactivity and Materials Design*, Cambridge University Press, 1986.
[16] G. Blasse, *Prog. Solid State Chem., 18* (1988) 79.
[17] R.M. Hazen, L.W. Finger and J.W. E. Mariathasan, *J. Phys. Chem. Solids, 46(2)* (1985) 253.
[18] G. Blasse, The luminescence of closed-shell transition-metal complexes: new developments, in *Structure and Bonding 42*, Springer-Verlag, Berlin, 1980.
[19] M. Sauvage, *Acta Crystallogr., B30* (1974) 2786.
[20] A. Ferretti, U.S. Patent 4,524,016, 1985.
[21] A.L. N. Stevels, *J. Luminesc., 12/13* (1976) 97.
[22] H. Haeuseler and M. Jung, *Mater. Res. Bull., 21* (1986) 1291.
[23] J.G. Rabatin, U.S. Patent 3,591,516, 1971.
[24] J.G. Rabatin, U.S. Patent 4,208,470, 1978.
[25] J.G. Rabatin, *Extended Abstracts of the Electrochem. Soc. Spring Meeting*, Toronto, Canada, Abstract no. 198 (1975) p. 467.
[26] H.A. Eick, *J. Am. Chem. Soc., 80* (1958) 43.
[27] B. Morosin and D.J. Newman, *Acta Crystallogr., B29* (1973) 2647.
[28] C.R. Ronda, H. Mulder and D.B. M. Klaassen, *J. Solid State Chem., 80* (1989) 299.
[29] L.H. Brixner and H.-y. Chen, *J. Electrochem. Soc., 130* (1983) 2435.
[30] J. Beutel, D.J. Mickewich, S.L. Issler and R. Shaw, *Phys. Med. Biol., 38* (1993) 1195.
[31] E.G. Saurborn, S.L. Issler, M. Yampolsky, J. Beutel and R. Shaw, *Soc. Photo-Optical Instrum. Eng. (SPIE), Phys. Med. Imaging, 1896* (1993) 314.
[32] J. Beutel, S.L. Issler, D.J. Mickewich and R. Shaw, *Soc. Photo-Optical Instrum. Eng. (SPIE), Phys. Med. Imaging, 2163* (1994) 36.
[33] D.B. Hedden, W.J. Zegarski and C.C. Torardi, *205th Am. Chem. Soc. National Meeting, Denver, Colorado, March/April 1993*, Inorganic Subdivision Abstract no. 240.
[34] D.B. Hedden, W.J. Zegarski and C.C. Torardi, *Extended Abstracts of the Electrochem. Soc. Fall Meeting*, New Orleans, LA, Abstract no. 473, 1993, p. 750.
[35] D.B. Hedden, C.C. Torardi and W. Zegarski, *J. Solid State Chem.*, in press.
[36] C.C. Torardi and C.R. Miao, to be published.
[37] R.S. Roth and J.L. Waring, *Am. Mineral., 48* (1963) 1348.
[38] Powder Diffraction File, JCPDS-International Centre for Diffraction Data, card 16-909 (1993).
[39] L.H. Brixner, *Mater. Res. Bull., 19* (1984) 143.
[40] M. Zocchi, M. Gatti, A. Santoro and R.S. Roth, *J. Solid State Chem., 48* (1983) 420.
[41] G. Blasse and A. Bril, *J. Electrochem. Soc., 115* (1968) 1067.
[42] K.D. Sieber, L.B. Todd and B.R. Sever, U.S. Patent 5,132,192, 1990.
[43] P.S. Bryan, P.M. Lambert, C.M. Towers and G.S. Jarrold, U.S. Patent 4,988,880, 1989.
[44] P.S. Bryan, P.M. Lambert, C.M. Towers and G.S. Jarrold, U.S. Patent 4,988,881, 1989.
[45] P.M. Lambert, P.S. Bryan, G.S. Jarrold and C.M. Towers, U.S. Patent 5,112,700, 1991.
[46] P.S. Bryan, L.C. Roberts, P.M. Lambert, C.M. Towers and G.S. Jarrold, *184th Electrochem. Soc. Meeting*, New Orleans, LA, October 1993, Abstract no. 475.
[47] P.S. Bryan, L.C. Roberts, P.M. Lambert, C.M. Towers and G.S. Jarrold, *184th Electrochem. Soc. Meeting*, New Orleans, LA, October 1993, Abstract no. 476.